



ARTICLE

Water-Based Environmentally Friendly Pesticide Formulations Based on Cyclodextrin/Pesticide Loading System

Xinyu Guo¹, Zhe Sun², Rui Zhao², Hongyi Shang², Jiangyu Liu², Yong Xu², Laihua Liu^{1,*} and Xuemin Wu^{2,*}

¹Key Lab of Plant-Soil Interaction, MOE, Center for Resources, Environment and Food Security, College of Resources and Environmental Sciences, China Agricultural University, Beijing, 100193, China

²Innovation Center of Pesticide Research, Department of Applied Chemistry, College of Science, China Agricultural University, Beijing, 100193, China

*Corresponding Authors: Laihua Liu. Email: LL1025@cau.edu.cn; Xuemin Wu. Email: wuxuemin@cau.edu.cn

This paper is dedicated to the 70th Anniversary of Pesticide Science in China Agricultural University

Received: 27 March 2022 Accepted: 19 May 2022

ABSTRACT

Difenoconazole (DIF) is a representative variety of broad-spectrum triazole fungicides and liposoluble pesticides. However, the water solubility of DIF is so poor that its application is limited in plant protection. In addition, the conventional formulations of DIF always contain abundant organic solvents, which may cause pollution of the environment. In this study, two DIF/cyclodextrins (CDs) inclusion complexes (ICs) were successfully prepared, which were DIF/ β -CD IC and DIF/hydroxypropyl- β -CD IC (DIF/HP- β -CD IC). The effect of cyclodextrins on the water solubility and the antifungal effect of liposoluble DIF pesticide were investigated. According to the phase solubility test, the molar ratio and apparent stability constant of ICs were obtained. Fourier transform infrared spectroscopy, thermal gravity analysis, X-ray diffraction and scanning electron microscopy were used systematically to characterize the formation and characteristics of ICs. The results noted that DIF successfully entered the cavities of two CDs. In addition, the antifungal effect test proved the better performance of DIF/HP- β -CD IC, which exceeded that of DIF emulsifiable concentrate. Therefore, our study provides informative direction for the intelligent use of liposoluble pesticides with cyclodextrins to develop water-based environmentally friendly formulations.

KEYWORDS

Water-based environmentally friendly pesticide formulations; difenoconazole; β -cyclodextrin; hydroxypropyl- β -cyclodextrin; inclusion complex; preparation; characterization

1 Introduction

In worldwide agricultural production, pesticides are very important substances by controlling diseases, insects, and weeds [1–3]. Most pesticides are inherently hydrophobic and liposoluble. Nearly all the active ingredients of pesticides cannot be used directly, requiring other additives to form formulations [4]. Owing to their limited water solubility, liposoluble pesticides are always processed into pesticide formulations using large quantities of organic solvents, surfactants, and carriers, such as emulsifiable concentrates (EC) and



wettable powder (WP) [5]. Conventional pesticide formulations can result in serious environmental and ecosystem problems [6]. Thus, the levels of organic solvents in pesticide formulations must be reduced, such as by improving the water solubility of liposoluble pesticides [7,8].

Difenoconazole (DIF) is a representative variety of broad-spectrum triazole fungicides and liposoluble pesticides developed by Giba Geigy in 1988 [9–11]. DIF destroys the fungal cell membrane by interfering with ergosterol biosynthesis [12,13]. As a broad-spectrum fungicide, DIF is applied worldwide in controlling diseases in vegetables, fruits, rice, and wheat [14–17]. However, the water solubility of DIF at 20°C is negligible ($15 \text{ mg}\cdot\text{L}^{-1}$) because of its structure as shown in Fig. 1 [18], it is usually formulated as EC, emulsion in water, and WP. Therefore, improving water solubility and formulating an environmentally friendly formulation of DIF is a promising approach to minimize the organic solvents and harm to the environment. Several studies have suggested that the formulation of cyclodextrins (CDs)/pesticides inclusion complexes (ICs) is an effective way for enhancing the water solubility of liposoluble pesticides [19,20].

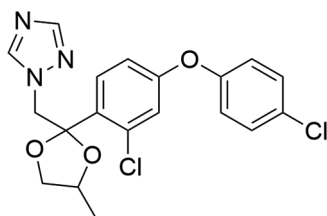


Figure 1: Structure of DIF

CDs are a series of cyclic oligosaccharides, which made up by at least six α -D-glucopyranose units and up to 12 α -D-glucopyranose units, as discovered in 1981 by Villiers from starch degradation [21,22]. At present, relevant research has focused on α -cyclodextrin (α -CD), β -cyclodextrin (β -CD), γ -cyclodextrin (γ -CD), and hydroxypropyl- β -cyclodextrin (HP- β -CD), which is the derivative of β -CD and has excellent solubility in water [23–25]. The cavity of CD molecules is hydrophobic, whereas the outer surface is hydrophilic [26,27]. Thus, hydrophobic molecules can enter the relatively hydrophobic cavities of CDs [28,29]. Therefore, as host molecules, CDs can enhance the water solubility of guest liposoluble molecules by forming ICs, thereby demonstrating the wide applicability of CDs in pesticides [30–32], medicines [33–35] and food [36–38].

In this study, as shown in Fig. 2, β -CD and HP- β -CD as host molecules were applied and DIF was applied as guest active ingredient to form DIF/CDs ICs. The saturated aqueous solution method and the freeze-drying method were successfully used to form DIF/ β -CD IC and DIF/HP- β -CD IC to ameliorate the physicochemical features of DIF, respectively. Fourier transform infrared spectroscopy (FTIR), thermal gravity analysis (TGA), X-ray diffraction (XRD) and scanning electron microscopy (SEM) were used systematically to characterize the formation and characteristics of two ICs. Antifungal effects of DIF ICs and traditional DIF ECs were compared using *Phytophthora infestans* (Mont.) de Bary and *Colletotrichum scovillei*. Our research offers valuable information for the improved utilization of DIF and CDs in liposoluble pesticides to develop water-based environmentally friendly formulations.

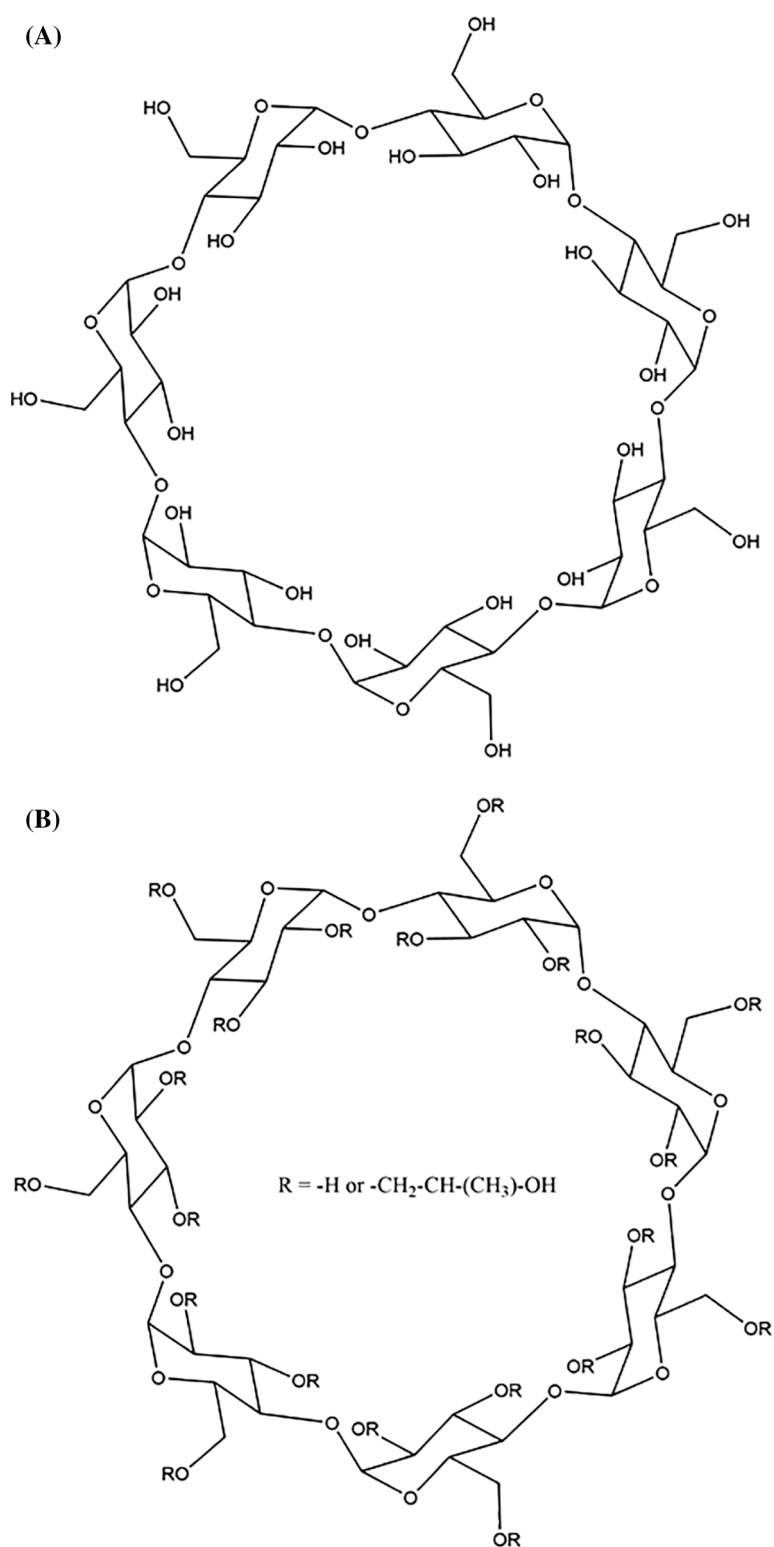


Figure 2: Structures of (A) β -CD and (B) HP- β -CD

2 Materials and Methods

2.1 Materials

DIF (MW \approx 406, 95.6% purity) and 250 g·L⁻¹ DIF EC were acquired from Zhejiang Udragon Bioscience Co., Ltd. (Hangzhou, China). Pure β -CD (MW \approx 1135) and HP- β -CD (MW \approx 1425) were purchased from Shandong Binzhou Zhiyuan Biotechnology Co., Ltd. (Binzhou, China). Anhydrous ethanol was purchased from Beijing Beihua Fine Chemicals Co., Ltd. (Beijing, China). *Phytophthora infestans* (Mont.) de Bary, *Colletotrichum scovillei*, potato dextrose agar (PDA), deionized water and sterilized water were obtained from the College of Science, China Agricultural University.

2.2 Phase Solubility Studies

Phase solubility studies were performed according to the previous literature based on Wang et al. [39] and García et al. [40]. First, 0.5 g DIF was weighed to 25 mL various concentrations aqueous solutions of β -CD or HP- β -CD (2, 4, 6, 8, 10, 12, 14 and 16 mM). The obtained suspensions were shaken on a thermostatic oscillator (THZ-C, Taicang, China) at 20°C for 24 h to achieve equilibrium between DIF and CDs. The suspensions were filtered with a 0.22 μ m syringe filter and diluted. The contents of DIF in filtrate solutions were analyzed by high-performance liquid chromatography (Agilent 1100, USA). By calculating and plotting, different solubilities of DIF in different aqueous solutions of CDs and phase solubility curves were obtained. From the phase solubility curves, the apparent stability constant (K_s) was calculated by the Eq. (1):

$$K_s = \frac{Slope}{S_0(1 - Slope)} \quad (1)$$

where S_0 is the solubility of DIF in deionized water without CDs at 20°C and *Slope* is the slope of the curves.

2.3 Preparation of ICs

DIF/ β -CD IC was made by the saturated aqueous solution method [41]. Briefly, the deionized water was used to dissolve 7.95 g β -CD at 50°C for 1 h to form a saturated aqueous solution. The desired amount of DIF (molar ratio of 1:1) was solubilized in anhydrous ethanol and added to above saturated aqueous solution drop by drop under magnetic stirring. The mixture was continuously stirred at 50°C for 8 h. The solution was stirred and cooled to 10°C for 12 h. The solid and liquid of the suspension was separated by Büchner funnel and anhydrous ethanol was used to wash the solid to remove free DIF. The last solid was vacuum-dried for 48 h to obtain DIF/ β -CD IC and for further studies.

DIF/HP- β -CD IC was made by the freeze-drying method [42]. Briefly, the deionized water was used to dissolve 9.98 g HP- β -CD at 50°C for 1 h to form an aqueous solution. The desired amount of DIF (molar ratio of 1:1) was solubilized in anhydrous ethanol and added to above aqueous solution drop by drop under magnetic stirring. The mixture was continuously stirred at 50°C for 8 h. The solution was stirred and cooled to 10°C for 12 h. The solid and liquid of the suspension was separated by Büchner funnel, and the liquid was lyophilized using a lyophilizer (FD-1C-50, Shanghai, China). Finally, DIF/HP- β -CD IC was obtained and used for further studies.

2.4 Preparation of Physical Mixtures (PMs)

PMs were prepared by simply mixing DIF and β -CD or DIF and HP- β -CD in a mortar for 30 min. The molar mixing ratio of CDs and DIF was 1:1. DIF/ β -CD PM and DIF/HP- β -CD PM were obtained and used for further studies.

2.5 Characterization of the Samples

DIF, CDs, ICs, and PMs were characterized using FTIR, XRD, TGA, and SEM.

2.5.1 FTIR Analysis

FTIR spectrometer (SHIMADZU IRTracer-100, Japan) was used to measure the FTIR spectra of different samples based on the KBr disk technique at 25°C. The scanning range was from 4000 to 400 cm⁻¹.

2.5.2 XRD Analysis

XRD analysis was studied from an X-ray powder diffractometer (Bruker D8 Focus, Germany). The XRD patterns were collected using Cu K α radiation (40 kV, 40 mA) at ambient temperature and an Ni filter between angular domain (2 θ) from 3° to 60°.

2.5.3 TGA

TGA was performed using a synchronous thermal analyzer (PerkinElmer STA6000, USA). 3–5 mg samples were weighed in crucibles. The experiment was performed under a high-purity nitrogen atmosphere at a flow rate of 100 mL·min⁻¹. The temperature range was from 25°C to 550°C and the heating rate was 10 °C·min⁻¹.

2.5.4 SEM Analysis

The SEM images of different samples were obtained using a SEM (Hitachi SU8010, Japan). Samples were put on a sample rack with aluminum strips, sputter-coated with gold, and then observed by SEM.

2.6 Antifungal Effect

The main fungi studied in this experiment were *Phytophthora infestans* (Mont.) de Bary and *Colletotrichum scovillei*, which are pathogenic fungi of potato late blight and pepper anthracnose, respectively. The antifungal effect of ICs and DIF EC was determined using the petri dish mycelial growth rate method in the laboratory. The experiment was carried out in the super clean platform. Different sample solutions of various concentrations were prepared in sterilized water. Thawed PDA (13.5 mL) were mixed with above solutions (1.5 mL) to obtain the DIF concentration of 0.01, 0.1, 0.5, 5.0, 50.0, and 500.0 mg·L⁻¹ in the ultimate solutions and poured into sterile petri dishes. When PDA with pesticide solutions were cool down and solidified, a 7 mm PDA with fungus was placed on each center of them. Then the sterile petri dishes were put in a constant temperature at 25°C and dark incubator for several days for the fungus growing. Finally, the mycelium diameter (mm) of each sample was obtained. PDA with sterilized water was applied as a control. Each concentration group was repeated three times. The growth inhibition rate I (%) was calculated by Eq. (2):

$$I(\%) = \frac{C - T}{C} \times 100 \quad (2)$$

where C is the average mycelium diameter (mm) of the control group; T is the average mycelium diameter (mm) of the DIF treatment groups. I (%) was transformed into a probability value. The toxicity regression equation was obtained from the relationship of probability value and logarithm of the DIF concentration. The concentration that inhibited 50% fungus growth (EC₅₀ values) for each formulation was calculated by the toxicity regression equation.

3 Results and Discussion

3.1 Phase Solubility Studies

Fig. 3 shows the phase solubility curves of DIF and CDs binary systems. There were positively correlated between the solubility of DIF and concentrations of CDs. The R² values were 0.98017 of β -CD with DIF and 0.99916 of HP- β -CD with DIF, indicating that the solubility of DIF and CDs concentrations have linear correlation. Based on the descriptions of Higuchi et al. [43] and Patel et al. [44], the curves can be considered as A_L type, which indicates that the molar ratio of inclusion of the

guest and host molecules is 1:1. Owing to the inclusion of CDs and DIF, the solubility of DIF in 16 mM solution of β -CD and HP- β -CD increased by 16.9 and 60.5 times, respectively.

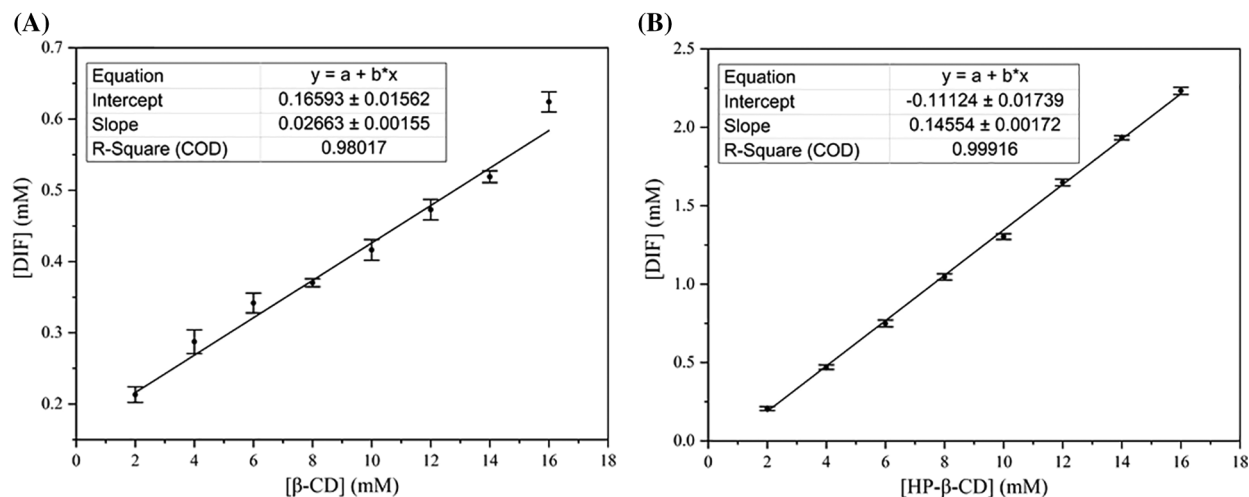


Figure 3: Phase solubility curves of DIF with (A) β -CD and (B) HP- β -CD

The K_s value, which could be determined by the phase solubility curves, represents binding strength of DIF onto the CD cavity. The suitable K_s value for ameliorating the physicochemical properties and bioactivity of liposoluble molecules is 200–5000 L·mol⁻¹ [45]. A low K_s value indicates the instability of the IC. Conversely, a high K_s value shows that the IC was firmly bound. The K_s value were 740.1 L·mol⁻¹ of DIF/ β -CD and 4475.1 L·mol⁻¹ of DIF/HP- β -CD. This suggests that DIF could be formed stable ICs with the two CDs. Moreover, HP- β -CD was tighter than β -CD in the combination with DIF. The results illustrated that CDs could significantly increase the solubility of DIF in water after inclusion, and the effect of HP- β -CD was better.

3.2 Samples Characterization

3.2.1 FTIR Analysis

Whether DIF enters the cavity of CDs can be proved by FTIR. In addition, there are a lot of useful information that can be applied to determine the formation of an IC, such as the shape, position, and strength of the characteristic peaks of the functional groups [46–48]. Fig. 4 shows the FTIR spectra of the different samples.

The stretching vibration (2977–3116 cm⁻¹) of the hydrocarbons on the benzene ring of DIF disappeared and the skeleton vibration (1585–1606 cm⁻¹) of the phenyl ring of DIF was obviously weakened in the two ICs. The C–O stretching vibration (1226 cm⁻¹) of DIF was weakened and shifted to 1236 and 1239 cm⁻¹ for DIF/ β -CD IC and DIF/HP- β -CD IC, respectively. For two PMs, the spectra exhibited the simple superpositions of DIF and CDs, indicating that the resulting compounds were simple mixtures. Therefore, DIF molecules were embedded in the cavity of two CDs, thereby forming ICs.

3.2.2 XRD Analysis

To identify the IC formation of DIF with CDs, XRD is always a useful method [49,50]. The changes of the characteristic diffraction peaks, including the new peaks emerging, the original peaks disappearing, and the peak intensity decaying, indicate the formation of ICs. The XRD patterns are shown in Fig. 5.

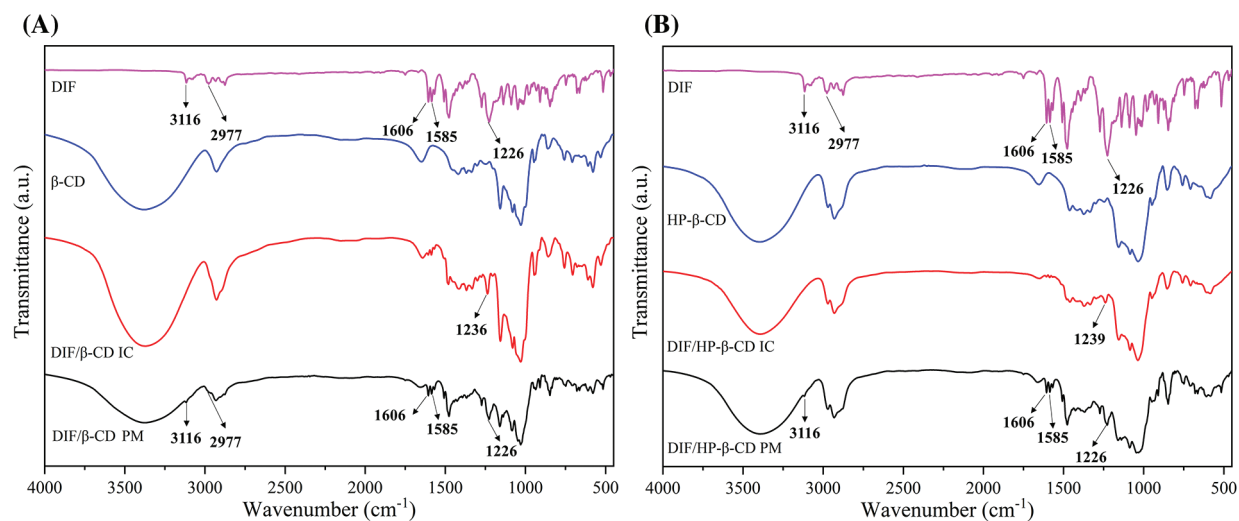


Figure 4: FTIR spectra of the (A) DIF/ β -CD and (B) DIF/HP- β -CD systems

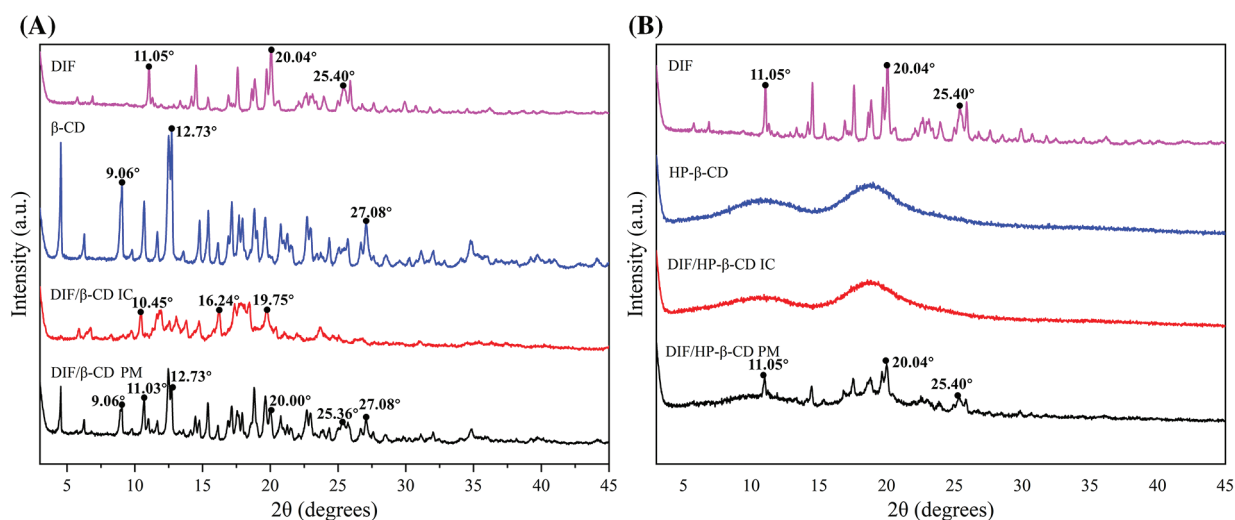


Figure 5: XRD patterns of the (A) DIF/ β -CD and (B) DIF/HP- β -CD systems

The DIF characteristic diffraction peaks are at $2\theta = 11.05^\circ$, 20.04° , and 25.40° , which are attributed to its crystal structure. In Fig. 5A, β -CD exhibits a crystalline nature with the salient peaks at 9.06° , 12.73° , and 27.08° . But for DIF/ β -CD PM, the diffraction peaks could be seen at 9.06° , 11.03° , 12.73° , 20.00° , 25.36° , and 27.08° , which include the peaks of two substances themselves, indicating that DIF/ β -CD IC could not be prepared by mixing the powders simply. In contrast, for DIF/ β -CD IC, the characteristic peaks are at $2\theta = 10.45^\circ$, 16.24° , and 19.75° , which are not present in other samples, indicating the successful formation of DIF/ β -CD IC. In Fig. 5B, HP- β -CD exhibits its amorphous structure with two broad diffraction peaks. However, DIF/HP- β -CD PM shows the notable characteristic diffraction peaks of DIF, indicating that the PM is a simple mixture of the two substances. In contrast, DIF/HP- β -CD IC exhibits its amorphous structure, similar with HP- β -CD, whereas the DIF peaks disappeared, indicating the successful formation of DIF/HP- β -CD IC. SEM can verify these results.

3.2.3 TGA

TGA can show the thermal properties of the samples and is an available method for determining the formation of ICs [51]. The TGA diagrams of the different samples are shown in Fig. 6.

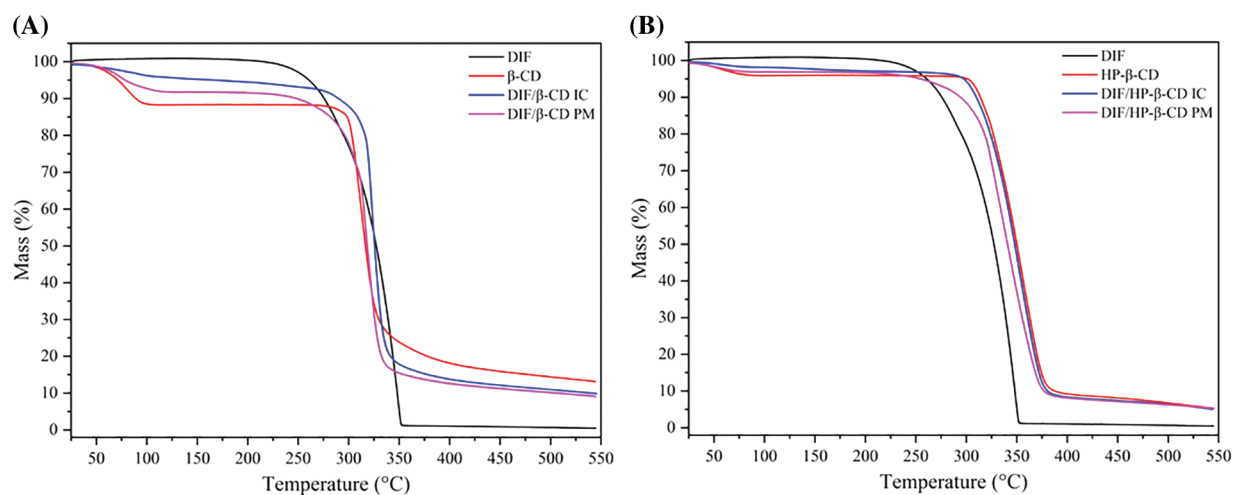


Figure 6: TGA thermograms of the (A) DIF/β-CD and (B) DIF/HP-β-CD systems

A single weightlessness process from 250°C to 350°C can be seen in the TGA thermogram of DIF. However, there are two weightlessness processes in the other samples, of which the first stages were attributed to the dehydration of CDs at 50°C–100°C. The second stage was attributed to the substance's degradation at 250°C–400°C for DIF/β-CD PM and at 250°C–375°C for DIF/HP-β-CD PM. For the two ICs, in the second stage, the temperatures at the beginning of the heat loss were higher than those of DIF and PMs, that is, 275°C and 300°C in DIF/β-CD IC and DIF/HP-β-CD IC, respectively, owing to the thermal decomposition of DIF at a higher temperature. The results indicated that ICs were formed between DIF and CDs, thereby improving the thermal stability of DIF.

3.2.4 SEM Analysis

The morphology of different samples can be shown visually by SEM, which is a powerful method to analyze the surface characteristics [52–54]. As shown in Fig. 7, the SEM images of different samples were compared to determine the formation of ICs. DIF exhibited a rough and irregular shape, β-CD had clear edges in a prismatic crystal, and HP-β-CD was mostly porous and spherical. For the PMs, the SEM images exhibited a simple mixture of DIF and CDs. For the ICs, the apparent appearance of the particles was completely different from that of the DIF and CDs. The morphology of DIF/β-CD IC comprised small new crystals, whereas that of DIF/HP-β-CD IC had almost no regular crystal morphology. We can see the similar results in the XRD. These results demonstrate the clear difference in the morphology of ICs, DIF, and CDs, indicating the successful formation of ICs.

3.3 Analysis of the Antifungal Effect Experiment

The petri dish mycelial growth rate method was used to evaluate the antifungal effect of the ICs and conventional formulations. The antifungal effect against *Phytophthora infestans* (Mont.) de Bary and *Colletotrichum scovillei* of the DIF/β-CD IC, DIF/HP-β-CD IC, and DIF EC systems are shown in Fig. 8 and Table 1.

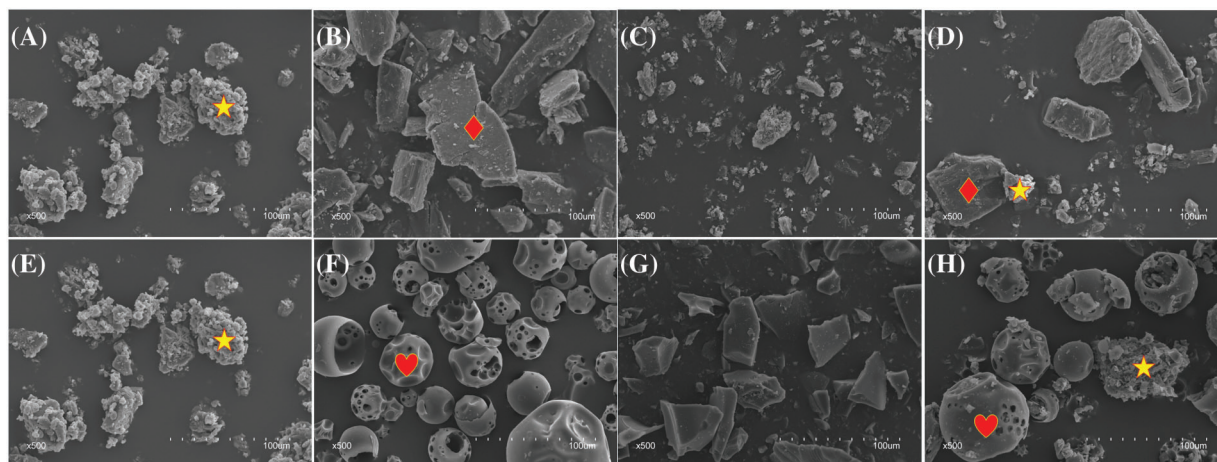


Figure 7: SEM images of (A,E) DIF, (B) β -CD, (C) DIF/ β -CD IC, (D) DIF/ β -CD PM, (F) HP- β -CD, (G) DIF/HP- β -CD IC, and (H) DIF/HP- β -CD PM

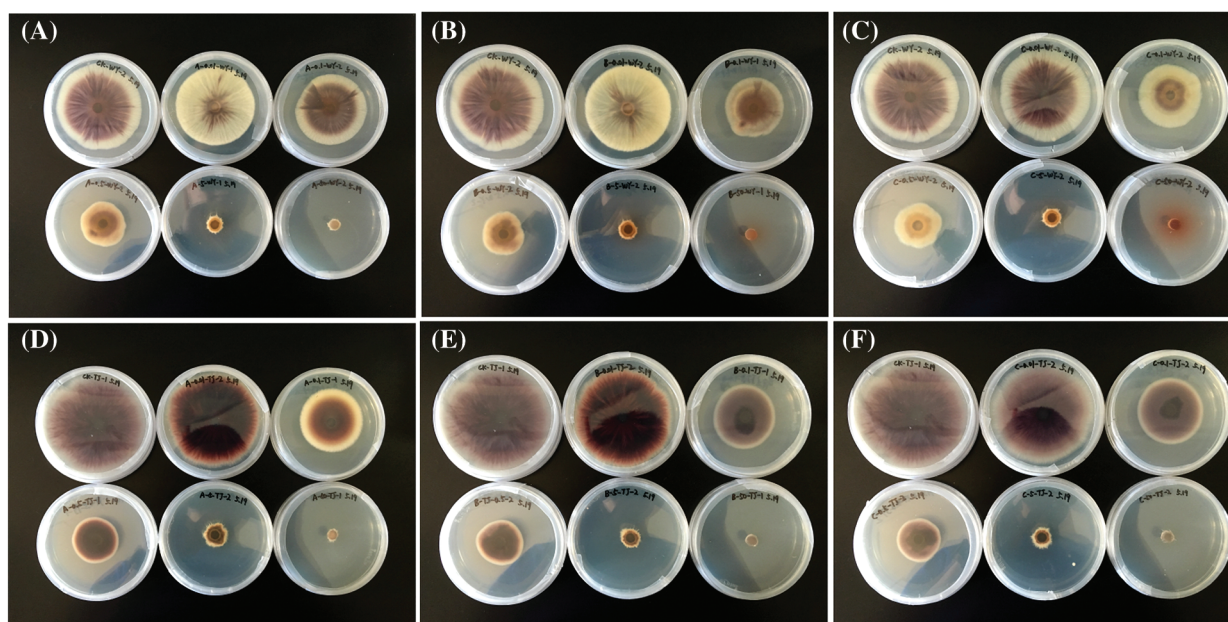


Figure 8: Antifungal effect against *Phytophthora infestans* (Mont.) de Bary and *Colletotrichum scovillei* of (A, D) DIF/ β -CD IC, (B, E) DIF/HP- β -CD IC, and (C, F) DIF EC. In each section, the concentrations of DIF were 0, 0.01, 0.1, 0.5, 5, and 50 $\text{mg}\cdot\text{L}^{-1}$

For the antifungal effect against *Phytophthora infestans* (Mont.) de Bary, the EC_{50} values of DIF/ β -CD IC, DIF/HP- β -CD IC and DIF EC were 0.451, 0.221, and 0.284 $\text{mg}\cdot\text{L}^{-1}$, respectively. The antifungal effect of DIF/HP- β -CD IC was better than those of DIF/ β -CD IC and DIF EC, with DIF/ β -CD IC having the poorest antifungal effect. For the antifungal effect against *Colletotrichum scovillei*, the EC_{50} values of DIF/ β -CD IC, DIF/HP- β -CD IC, and DIF EC were 0.199, 0.149 and 0.144 $\text{mg}\cdot\text{L}^{-1}$, respectively. The results showed that the antifungal effect of DIF/HP- β -CD IC was better than that of DIF/ β -CD IC and equivalent to that of DIF EC. This was consistent with the antifungal effect results against *Phytophthora infestans* (Mont.) de Bary. In

summary, due to the inclusion complex of DIF and CDs, the solubility of DIF in water was improved, which enhanced the fungicidal effect of DIF to varying degrees.

Table 1: Toxicity equations and EC₅₀ of DIF/β-CD IC, DIF/HP-β-CD IC, and DIF EC against *Phytophthora infestans* (Mont.) de Bary and *Colletotrichum scovillei*

<i>Phytophthora infestans</i> (Mont.) de Bary			
	Toxicity equation	R-square (COD)	EC ₅₀ (mg·L ⁻¹)
DIF/β-CD IC	$y = 5.3812 + 1.1022x$	0.9920	0.451
DIF/HP-β-CD IC	$y = 5.7783 + 1.1856x$	0.9938	0.221
DIF EC	$y = 5.6277 + 1.1471x$	0.9782	0.284
<i>Colletotrichum scovillei</i>			
	Toxicity equation	R-square (COD)	EC ₅₀ (mg·L ⁻¹)
DIF/β-CD IC	$y = 5.6411 + 0.9150x$	0.9972	0.199
DIF/HP-β-CD IC	$y = 5.7779 + 0.9412x$	0.9888	0.149
DIF EC	$y = 5.7476 + 0.8890x$	0.9874	0.144

4 Conclusions

In this study, DIF/β-CD IC and DIF/HP-β-CD IC were formed to increase the solubility of DIF by the saturated aqueous solution method and the freeze-drying method, respectively. According to the phase solubility method, the 1:1 molar ratio and apparent stability constant of ICs were calculated. FTIR, TGA, XRD and SEM were applied to prove ICs formation. The results indicate the successful formation of ICs. For the antifungal effect test, the effect against *Phytophthora infestans* (Mont.) de Bary and *Colletotrichum scovillei* of DIF/HP-β-CD IC was better than that of DIF/β-CD, and was comparable to that of DIF EC. Our research not only provides informative direction for the intelligent use of liposoluble pesticides for reducing the amount of organic solvent used, but also shows that CDs can be utilized in liposoluble pesticides to develop water-based environmentally friendly formulations.

Funding Statement: The authors received no specific funding for this study.

Conflicts of Interest: The authors declare that they have no conflicts of interest to report regarding the present study.

References

1. Artusio, F., Casà, D., Granetto, M., Tosco, T., Pisano, R. (2021). Alginate nanohydrogels as a biocompatible platform for the controlled release of a hydrophilic herbicide. *Processes*, 9(9), 1641. DOI 10.3390/pr9091641.
2. Kong, X. P., Zhang, B. H., Wang, J. (2021). Multiple roles of mesoporous silica in safe pesticide application by nanotechnology: A review. *Journal of Agricultural and Food Chemistry*, 69(24), 6735–6754. DOI 10.1021/acs.jafc.1c01091.
3. Sharma, A., Kumar, V., Shahzad, B., Tanveer, M., Sidhu, G. P. S. et al. (2019). Worldwide pesticide usage and its impacts on ecosystem. *SN Applied Sciences*, 1, 1446. DOI 10.1007/s42452-019-1485-1.
4. Alavanja, M. C. R. (2009). Introduction: Pesticides use and exposure, extensive worldwide. *Reviews on Environmental Health*, 24(4), 303–309. DOI 10.1015/REVEH.2009.24.4.303.

5. Zhao, X., Cui, H., Wang, Y., Sun, C., Cui, B. et al. (2018). Development strategies and prospects of nano-based smart pesticide formulation. *Journal of Agricultural and Food Chemistry*, 66(26), 6504–6512. DOI 10.1021/acs.jafc.7b02004.
6. Song, S., Jiang, X., Shen, H., Wu, W., Shi, Q. et al. (2021). MXene (Ti₃C₂) based pesticide delivery system for sustained release and enhanced pest control. *ACS Applied Bio Materials*, 4(9), 6912–6923. DOI 10.1021/acsabm.1c00607.
7. Geng, Q., Xie, J., Wang, X., Cai, M., Ma, H. et al. (2018). Preparation and characterization of butachlor/(2-hydroxypropyl)- β -cyclodextrin inclusion complex: Improve soil mobility and herbicidal activity and decrease fish toxicity. *Journal of Agricultural and Food Chemistry*, 66(46), 12198–12205. DOI 10.1021/acs.jafc.8b04812.
8. Gao, S., Jiang, J. Y., Liu, Y. Y., Fu, Y., Zhao, L. X. et al. (2019). Enhanced solubility, stability, and herbicidal activity of the herbicide diuron by complex formation with β -cyclodextrin. *Polymers*, 11(9), 1396. DOI 10.3390/polym11091396.
9. Huang, S., Yan, W., Liu, M., Hu, J. (2016). Detection of difenoconazole pesticides in pak choi by surface-enhanced Raman scattering spectroscopy coupled with gold nanoparticles. *Analytical Methods*, 8(23), 4755–4761. DOI 10.1039/c6ay00513f.
10. Li, J., Dong, F., Cheng, Y., Liu, X., Xu, J. et al. (2012). Simultaneous enantioselective determination of triazole fungicide difenoconazole and its main chiral metabolite in vegetables and soil by normal-phase high-performance liquid chromatography. *Analytical and Bioanalytical Chemistry*, 404, 2017–2031. DOI 10.1007/s00216-012-6240-z.
11. Chen, S., Cai, L., Zhang, H., Zhang, Q., Song, J. et al. (2021). Deposition distribution, metabolism characteristics, and reduced application dose of difenoconazole in the open field and greenhouse pepper ecosystem. *Agriculture, Ecosystems and Environment*, 313, 107370. DOI 10.1016/j.agee.2021.107370.
12. Liu, B., Feng, J., Sun, X., Sheng, W., Zhang, Y. et al. (2018). Development of an enzyme-linked immunosorbent assay for the detection of difenoconazole residues in fruits and vegetables. *Food Analytical Methods*, 11, 119–127. DOI 10.1007/s12161-017-0983-2.
13. Khwanes, S. A., Mohamed, R. A., Ibrahim, K. A., El-Rahman, H. A. A. (2022). Ginger reserves testicular spermatogenesis and steroidogenesis in difenoconazole-intoxicated rats by conducting oxidative stress, apoptosis and proliferation. *Andrologia*, 54, e14241. DOI 10.1111/and.14241.
14. Zhu, J., Liu, C., Wang, J., Liang, Y., Gong, X. et al. (2021). Difenoconazole induces cardiovascular toxicity through oxidative stress-mediated apoptosis in early life stages of zebrafish (*Danio rerio*). *Ecotoxicology and Environmental Safety*, 216, 112227. DOI 10.1016/j.ecoenv.2021.112227.
15. Zhao, F., Liu, J., Xie, D., Lv, D., Luo, J. (2018). A novel and actual mode for study of soil degradation and transportation of difenoconazole in a mango field. *RSC Advances*, 8(16), 8671–8677. DOI 10.1039/c8ra00251g.
16. Wang, K., Sun, D. W., Pu, H., Wei, Q. (2019). Surface-enhanced Raman scattering of core-shell Au@Ag nanoparticles aggregates for rapid detection of difenoconazole in grapes. *Talanta*, 191, 449–456. DOI 10.1016/j.talanta.2018.08.005.
17. Pereira, V. R., Pereira, D. R., Vieira, K. C. D. M. T., Ribas, V. P., Constantino, C. J. L. et al. (2019). Sperm quality of rats exposed to difenoconazole using classical parameters and surface-enhanced Raman scattering: Classification performance by machine learning methods. *Environmental Science and Pollution Research*, 26, 35253–35265. DOI 10.1007/s11356-019-06407-0.
18. Khalaf, B., Hamed, O., Jodeh, S., Bol, R., Hanbali, G. et al. (2021). Cellulose-based hectocycle nanopolymers: Synthesis, molecular docking and adsorption of difenoconazole from aqueous medium. *International Journal of Molecular Sciences*, 22, 6090. DOI 10.3390/ijms22116090.
19. Shen, C., Yang, X., Wang, Y., Zhou, J., Chen, C. (2012). Complexation of capsaicin with β -cyclodextrins to improve pesticide formulations: Effect on aqueous solubility, dissolution rate, stability and soil adsorption. *Journal of Inclusion Phenomena Macrocyclic Chemistry*, 72(3), 263–274. DOI 10.1007/s10847-011-9971-0.
20. Garrido, J., Cagide, F., Melle-Franco, M., Borges, F., Garrido, E. M. (2014). Microencapsulation of herbicide MCPA with native β -cyclodextrin and its methyl and hydroxypropyl derivatives: An experimental and theoretical investigation. *Journal of Molecular Structure*, 1061, 76–81. DOI 10.1016/j.molstruc.2013.12.067.

21. Velázquez-Contreras, F., Zamora-Ledezma, C., López-González, I., Meseguer-Olmo, L., Núñez-Delicado, E. et al. (2022). Cyclodextrins in polymer-based active food packaging: A fresh look at nontoxic, biodegradable, and sustainable technology trends. *Polymers*, *14*(1), 104. DOI 10.3390/polym14010104.
22. Arruda, T. R., Marques, C. S., Soares, N. F. F. (2021). Native cyclodextrins and their derivatives as potential additives for food packaging: A review. *Polysaccharides*, *2*(4), 825–842. DOI 10.3390/polysaccharides2040050.
23. Liu, Y., Sameen, D. E., Ahmed, S., Wang, Y., Lu, R. et al. (2022). Recent advances in cyclodextrin-based films for food packaging. *Food Chemistry*, *370*, 131026. DOI 10.1016/j.foodchem.2021.131026.
24. Wang, J. W., Yu, K. X., Ji, X. Y., Bai, H., Zhang, W. H. et al. (2021). Structural insights into the host–guest complexation between β -cyclodextrin and bio-conjugatable adamantane derivatives. *Molecules*, *26*(9), 2412. DOI 10.3390/molecules26092412.
25. Wu, H. T., Chuang, Y. H., Lin, H. C., Chien, L. J. (2021). Characterization and aerosolization performance of hydroxypropyl-beta-cyclodextrin particles produced using supercritical assisted atomization. *Polymers*, *13*(14), 2260. DOI 10.3390/polym13142260.
26. Pereva, S., Himitliiska, T., Spassov, T., Stoyanov, S. D., Arnaudov, L. N. et al. (2015). Cyclodextrin-based solid–gas clathrates. *Journal of Agricultural and Food Chemistry*, *63*(29), 6603–6613. DOI 10.1021/acs.jafc.5b01357.
27. Usacheva, T. R., Volynkin, V. A., Panyushkin, V. T., Lindt, D. A., Pham, T. L. et al. (2021). Complexation of cyclodextrins with benzoic acid in water-organic solvents: A solvation-thermodynamic approach. *Molecules*, *26*(15), 4408. DOI 10.3390/molecules26154408.
28. Tian, B., Xiao, D., Hei, T., Ping, R., Hua, S. et al. (2020). The application and prospects of cyclodextrin inclusion complexes and polymers in the food industry: A review. *Polymer International*, *69*, 597–603. DOI 10.1002/pi.5992.
29. Kfoury, M., Landy, D., Fourmentin, S. (2018). Characterization of cyclodextrin/volatile inclusion complexes: A review. *Molecules*, *23*(5), 1204. DOI 10.3390/molecules23051204.
30. Schirra, M., Delogu, G., Cabras, P., Angioni, A., D'hallewin, G. et al. (2002). Complexation of imazalil with β -cyclodextrin, residue uptake, persistence, and activity against penicillium decay in citrus fruit following postharvest dip treatments. *Journal of Agricultural and Food Chemistry*, *50*(23), 6790–6797. DOI 10.1021/jf020542v.
31. Loron, A., Gardrat, C., Tabary, N., Martel, B., Coma, V. (2021). Tetrahydrocurcumin encapsulation in cyclodextrins for water solubility improvement: Synthesis, characterization and antifungal activity as a new biofungicide. *Carbohydrate Polymer Technologies and Applications*, *2*, 100113. DOI 10.1016/j.carpta.2021.100113.
32. Zhu, X. L., Wang, H. B., Chen, Q., Yang, W. C., Yang, G. F. (2007). Preparation and characterization of inclusion complex of iprodione and β -cyclodextrin to improve fungicidal activity. *Journal of Agricultural and Food Chemistry*, *55*(9), 3535–3539. DOI 10.1021/jf070197f.
33. Krzak, A., Swiech, O., Majdecki, M., Garbacz, P., Gwardys, P. et al. (2021). Adjusting the structure of β -cyclodextrin to improve complexation of anthraquinone-derived drugs. *Molecules*, *26*(23), 7205. DOI 10.3390/molecules26237205.
34. Celebioglu, A., Uyar, T. (2019). Metronidazole/hydroxypropyl- β -cyclodextrin inclusion complex nanofibrous webs as fast-dissolving oral drug delivery system. *International Journal of Pharmaceutics*, *572*, 118828. DOI 10.1016/j.ijpharm.2019.118828.
35. Mashaqbeh, H., Obaidat, R., Al-Shar'i, N. (2021). Evaluation and characterization of curcumin- β -cyclodextrin and cyclodextrin-based nanosponge inclusion complexation. *Polymers*, *13*(23), 4073. DOI 10.3390/polym13234073.
36. Cui, H., Bai, M., Lin, L. (2018). Plasma-treated poly(ethylene oxide) nanofibers containing tea tree oil/ β -cyclodextrin inclusion complex for antibacterial packaging. *Carbohydrate Polymers*, *179*, 360–369. DOI 10.1016/j.carbpol.2017.10.011.
37. Cid-Samamed, A., Rakmai, J., Mejuto, J. C., Simal-Gandara, J., Astray, G. (2022). Cyclodextrins inclusion complex: Preparation methods, analytical techniques and food industry applications. *Food Chemistry*, *384*, 132467. DOI 10.1016/j.foodchem.2022.132467.
38. Lin, Y., Huang, R., Sun, X., Yu, X., Xiao, Y. et al. (2022). The p-anisaldehyde/ β -cyclodextrin inclusion complexes as a sustained release agent: Characterization, storage stability, antibacterial and antioxidant activity. *Food Control*, *132*, 108561. DOI 10.1016/j.foodcont.2021.108561.

39. Wang, L., Li, S., Tang, P., Yan, J., Xu, K. et al. (2015). Characterization and evaluation of synthetic riluzole with β -cyclodextrin and 2,6-di-*O*-methyl- β -cyclodextrin inclusion complexes. *Carbohydrate Polymers*, 129, 9–16. DOI 10.1016/j.carbpol.2015.04.046.
40. García, A., Leonardi, D., Salazar, M. O., Lamas, M. C. (2014). Modified β -cyclodextrin inclusion complex to improve the physicochemical properties of albendazole. Complete *in vitro* evaluation and characterization. *PLoS One*, 9(2), e88234. DOI 10.1371/journal.pone.0088234.
41. Ren, X., Yue, S., Xiang, H., Xie, M. (2018). Inclusion complexes of eucalyptus essential oil with β -cyclodextrin: Preparation, characterization and controlled release. *Journal of Porous Materials*, 25, 1577–1586. DOI 10.1007/s10934-018-0571-x.
42. Guan, T., Zhang, G., Sun, Y., Zhang, J., Ren, L. (2021). Preparation, characterization, and evaluation of HP- β -CD inclusion complex with alcohol extractives from star anise. *Food & Function*, 12, 10008–10022. DOI 10.1039/d1fo02097h.
43. Higuchi, T., Connors, K. A. (1965). Phase solubility techniques. *Advances in Analytical Chemistry and Instrumentation*, 4(2), 117–212.
44. Patel, M., Hirlekar, R. (2019). Multicomponent cyclodextrin system for improvement of solubility and dissolution rate of poorly water soluble drug. *Asian Journal of Pharmaceutical Sciences*, 14(1), 104–115. DOI 10.1016/j.ajps.2018.02.007.
45. Amruta, T., Nancy, P., Prashant, K., Niteshkumar, S. (2018). Encapsulation of boswellic acid with β - and hydroxypropyl- β -cyclodextrin: Synthesis, characterization, *in vitro* drug release and molecular modelling studies. *Journal of Molecular Structure*, 1154, 504–510. DOI 10.1016/j.molstruc.2017.10.061.
46. Cai, C., Ma, R., Duan, M., Lu, D. (2019). Preparation and antimicrobial activity of thyme essential oil microcapsules prepared with gum arabic. *RSC Advances*, 9(34), 19740–19747. DOI 10.1039/c9ra03323h.
47. Rodrigues, S. G., Chaves, I. D. S., de Melo, N. F. S., de Jesus, M. B., Fraceto, L. F. et al. (2011). Computational analysis and physico-chemical characterization of an inclusion compound between praziquantel and methyl- β -cyclodextrin for use as an alternative in the treatment of schistosomiasis. *Journal of Inclusion Phenomena Macrocyclic Chemistry*, 70(1), 19–28. DOI 10.1007/s10847-010-9852-y.
48. Li, Q., Gong, S., Yan, J., Hu, H., Shu, X. et al. (2020). Synthesis and kinetics of hydrogenated rosin dodecyl ester as an environment friendly plasticizer. *Journal of Renewable Materials*, 8(3), 289–300. DOI 10.32604/jrm.2020.08897.
49. Li, W., Liu, X., Yang, Q., Zhang, N., Du, Y. et al. (2015). Preparation and characterization of inclusion complex of benzyl isothiocyanate extracted from papaya seed with β -cyclodextrin. *Food Chemistry*, 184, 99–104. DOI 10.1016/j.foodchem.2015.03.091.
50. Li, F., Yang, W., Kong, L., Hong, H., Liao, X. et al. (2019). Host-guest inclusion systems of podophyllotoxin with β -cyclodextrin derivatives for low cytotoxicity. *Journal of Drug Delivery Science Technology*, 54, 101280. DOI 10.1016/j.jddst.2019.101280.
51. Chouker, M. A., Abdallah, H., Zeiz, A., El-Dakdouki, M. (2021). Host-guest inclusion complex of quinoxaline-1, 4-dioxide derivative with 2-hydroxypropyl- β -cyclodextrin: Preparation, characterization, and antibacterial activity. *Journal of Molecular Structure*, 1235, 130273. DOI 10.1016/j.molstruc.2021.130273.
52. Li, Q., Yan, X., Chen, J., Shu, X., Jia, P. et al. (2021). Preparation and characterization of potassium monopersulfate/ethyl cellulose microcapsules and their sustained release performance. *Journal of Renewable Materials*, 9(10), 1673–1684. DOI 10.32604/jrm.2021.014695.
53. Gu, W., Liu, Y. (2020). Characterization and stability of beta-acids/hydroxypropyl- β -cyclodextrin inclusion complex. *Journal of Molecular Structure*, 1201, 127159. DOI 10.1016/j.molstruc.2019.127159.
54. Prabu, S., Swaminathan, M., Sivakumar, K., Rajamohan, R. (2015). Preparation, characterization and molecular modeling studies of the inclusion complex of caffeine with beta-cyclodextrin. *Journal of Molecular Structure*, 1099, 616–624. DOI 10.1016/j.molstruc.2015.07.018.